INORGANIC CHEMISTRY FRONTIERS

RESEARCH ARTICLE

View Article Online
View Journal | View Issue

Cite this: *Inorg. Chem. Front.*, 2023, **10**, 5622

Synthesis and reactivity of a uranium(IV) complex supported by a monoanionic nitrogen–phosphorus ligand†

Kai Li, Jialu He, Yue Zhao and Congqing Zhu *

A monoanionic nitrogen–phosphorus ligand $(CH_3)_2NCH_2CH_2NHP^iPr_2$ (**L3**) was designed and the corresponding U(IV) chloride complex $\{[(CH_3)_2NCH_2CH_2NP^iPr_2]_2UCl_2\}$ (**1**) and U(IV) iodide complex $\{[(CH_3)_2NCH_2CH_2NP^iPr_2]_2UI_2\}$ (**2**) were readily synthesized. Complexes **1** and **2** were fully characterized and the reactivity of complex **1** was further investigated. Complex **3** $\{[(CH_3)_2NCH_2CH_2NP^iPr_2]_2U(C_{12}H_8)\}$ with a uranium cyclopentadiene unit was constructed by the reaction of **1** with 2,2′-dilithiobiphenyl, which is a rare example of a homoleptic metallafluorene containing an actinide element. In addition, a U(IV) bi-alkyl complex $\{[(CH_3)_2NCH_2CH_2NP^iPr_2]_2U[o\text{-}N(CH_3)(CH_2)C_6H_4CH_2]\}$ (**4**) was isolated by the reaction of complex **1** with two equivalents of $o\text{-}N(CH_3)_2C_6H_4CH_2K$. Moreover, the reactivity of **1** with a series of transition metal precursors was also investigated, from which heterometallic clusters $\{[(CH_3)_2NCH_2CH_2NP^iPr_2]_2UCl_2(\mu\text{-}Cl)RuCl\}_2$ (**5**), $\{[(CH_3)_2NCH_2CH_2NP^iPr_2]_2UCl_2Rh(\mu\text{-}Cl)\}_2$ (**6**) and $\{[(CH_3)_2NCH_2CH_2NP^iPr_2]_2UCl_2Ir(\mu\text{-}Cl)\}_2$ (**7**) were isolated. The U–Rh and U–Ir single bonds were observed in complexes **6** and **7**, respectively. This study further confirms that the nitrogen–phosphorus ligand is an effective platform for the construction of species with U–M bonds.

Received 25th July 2023,
Accepted 17th August 2023

DOI: 10.1039/d3qi01447a

rsc.li/frontiers-inorganic

Introduction

Ligands are important in organometallic chemistry because of their significant influence on the structure and properties of organometallic complexes.[1,2] The synthesis of ferrocene supported by the cyclopentadienyl (Cp) ligand was considered to be a starting point of modern organometallic chemistry.[3] The first example of a uranium organometallic complex, Cp_3UCl, was also stabilized by the Cp ligand.[4] Based on hard–soft acid–base theory, the N and O atoms are good donors to actinide elements. Consequently, a series of new ligands with N and O coordination sites were designed and used in the development of actinide organometallic chemistry.[5–18] For instance, since the first example of an actinide complex supported by a triamidoamine ($[(RNCH_2CH_2)_3N]^{3-}$) ligand (Tren) was reported by Scott and co-workers in 1994,[19] actinide organometallic chemistry with Tren ligands has flourished.[18,20–26] With these trianionic ligands, a series of trivalent uranium complexes were isolated.[24,25,27,28]

In 2019, we found that a novel phosphine-substituted Tren ligand (**L1**, Fig. 1), namely a double-layer N–P ligand, can also be used to stabilize uranium(III) complexes and construct a series of heterometallic clusters with multiple U–M single or triple bonds.[29–31] In a subsequent study, we found that the dianionic double-layer N–P ligand (**L2**, Fig. 1) is an effective platform for the construction of heterometallic clusters with multiple U–M single or double bonds and could be used to synthesize neutral uranium(II) species.[32–34] In 2022, Layfield and co-workers reported the first example of a uranium(I) complex supported by a monoanionic ligand, $\eta^5\text{-}C_5{}^iPr_5$.[35] Very recently, Mazzanti and co-workers found that the $-OSiPh_3$ ligand could be used to stabilize uranium(I) synthons.[36] These U(I) complexes are ionic-type species supported by multiple monoanionic ligands. Therefore, we are curious if a neutral U(I) species could be stabilized by a monoanionic ligand with additional

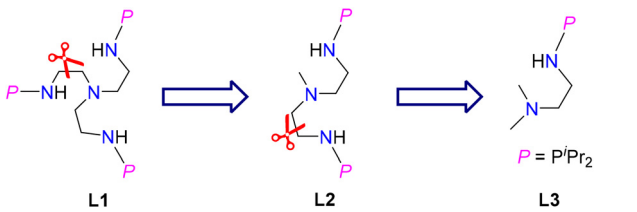

Fig. 1 Design of the monoanionic N–P ligand **L3**.

State Key Laboratory of Coordination Chemistry, Jiangsu Key Laboratory of Advanced Organic Materials, School of Chemistry and Chemical Engineering, Nanjing University, Nanjing 210023, China. E-mail: zcq@nju.edu.cn

†Electronic supplementary information (ESI) available. CCDC 2254126–2254132. For ESI and crystallographic data in CIF or other electronic format see DOI: https://doi.org/10.1039/d3qi01447a

donor coordination sites. Based on our continuing interest in uranium chemistry supported by N–P ligands,[37–43] herein, we have designed a new monoanionic double-layer N–P ligand with a pendant dimethylamino group as an additional coordination site (**L3**, Fig. 1). However, an unanticipated uranium precursor (**1**) supported by two **L3** ligands was isolated. The reactivity of complex **1** was investigated in this study. Interestingly, the two P atoms from two **L3** ligands in complex **1** could be coordinated with the same transition metal, which is totally different from the heterometallic clusters with multiple U–M bonds supported by **L1** and **L2**.

Results and discussion

Synthesis of U(IV) complexes 1 and 2

The monoanionic ligand **L3** was prepared from the reaction of *N*,*N*-dimethylethylenediamine with one equivalent of $^{i}Pr_2PCl$ in the presence of excess Et_3N (see the ESI for details†). **L3** was deprotonated with ^{n}BuLi at 25 °C in THF for 3 h and then treated with UCl_4 overnight at room temperature (RT) (Scheme 1), from which complex **1** was isolated as a bright-green solid in 78% yield after recrystallization from toluene at −30 °C. We found that different equivalents of **L3** do not change the product in this reaction.

Under similar conditions, deprotonated **L3** could also react with $UI_3(THF)_4$,[44] leading to the formation of U(IV) complex **2** in 37% yield as a crystalline product (Scheme 1). We proposed that a U(III) complex supported by **L3** was formed and disproportionated into U(IV) complex **2** and U(0) species, a phenomenon which has been observed previously.[45–48] Complex **2** could also be synthesized in 91% yield by the reaction of complex **1** with TMSI. The reactions forming complexes **1** and **2** are different from the reactions leading to tri- and tetra-substituted U(IV) products containing isopropyl (^{i}Pr) and mestrimethylphenyl (Mes)-substituted monoanionic N–P ligands, $^{i}PrNHPPh_2$ and $MesNHP^{i}Pr_2$, which were reported by Bart, Thomas and co-workers.[49] This difference is probably due to the additional NMe_2 group that could be coordinated with the U center, thus avoiding the formation of tri- and tetra-substituted U(IV) products.

The ^{1}H NMR spectra of complexes **1** and **2** exhibit five signals between +58.0 and −74.4 ppm, consistent with reported U(IV) complexes supported by dianionic N–P ligands.[32,33] The signals for N–CH_3 in complexes **1** and **2** were observed at −70.5 and −74.4 ppm, respectively. No phosphorus signals were observed between +1000 and −1000 ppm, probably due to the paramagnetic nature of U(IV) species.

The molecular structure of complexes **1** and **2** was confirmed by single-crystal X-ray diffraction. As shown in Fig. 2 and 3, the uranium centre of these species is octa-coordinated with four N atoms and two P atoms from two monoanionic N–P ligands, and two halogen atoms. In complex **1**, the bond lengths of U–N_{amine} (U1–N1: 2.698(4) Å, U1–N3: 2.691(4) Å) are obviously longer than those of U–N_{amido} (U1–N2: 2.249(4) Å, U1–N4: 2.248(4) Å), reflecting the dative bonds between the U center and N1 and N3. The bond lengths of U1–P1 (3.0042(14) Å) and U1–P2 (2.9589(14) Å) are longer than the sum of the covalent single-bond radii of U and P (2.80 Å),[50] suggesting a weak coordination between the two P atoms and the U center. The structural parameters of complex **2** are comparable to those of complex **1**.

Synthesis of uranium bi-aryl complex 3 and uranium bi-alkyl complex 4

Compared with uranium alkyl complexes, uranium aryl complexes remain extremely rare.[51–54] The first example of a homoleptic uranium aryl complex was reported by Arnold in 2016.[55] Reported uranium aryl complexes feature one or more monoaryl units, whereas uranium bi-aryl complexes have not been reported. Heterofluorenes, in which the CH_2 unit in fluorene was replaced by a heteroatom, have been reported for several decades. Heteroatoms in the heterofluorenes could be main group elements,[56,57] transition metals,[58,59] and rare-earth metals.[60,61] With complex **1** in hand, we attempted to synthesize a uranium-containing metallafluorene species *via* salt

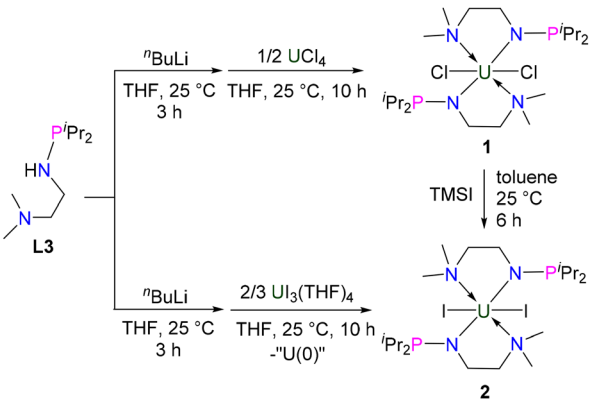

Scheme 1 Synthesis of complexes **1** and **2**.

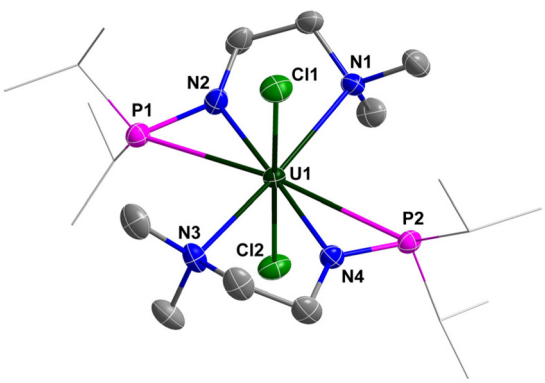

Fig. 2 Molecular structure of **1** with thermal ellipsoids at the 50% probability level. Hydrogen atoms are omitted for clarity. The ^{i}Pr groups on P atoms are simplified into lines. Selected bond distances (Å): U1–N1 2.698(4), U1–N2 2.249(4), U1–N3 2.691(4), U1–N4 2.248(4), U1–P1 3.0042(14), U1–P2 2.9589(14), U1–Cl1 2.6890(13), U1–Cl2 2.6856(13).

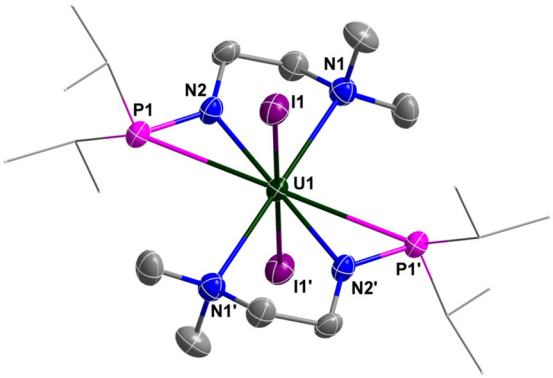

Fig. 3 Molecular structure of **2** with thermal ellipsoids at the 50% probability level. Hydrogen atoms are omitted for clarity. The ^{i}Pr groups on P atoms are simplified into lines. Selected bond distances (Å): U1–N1 2.737(4), U1–N2 2.237(4), U1–P1 2.9694(11), U1–I1 3.1109(3).

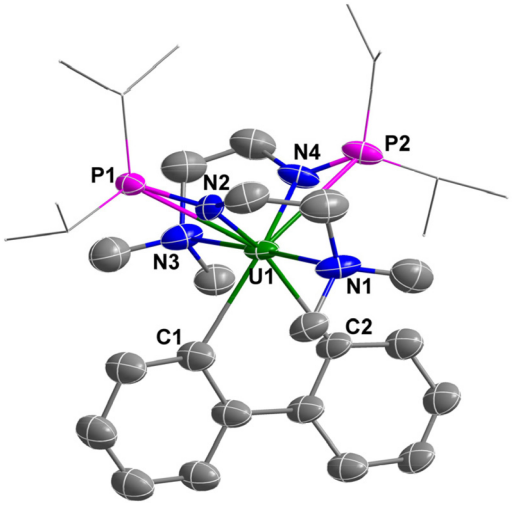

Fig. 4 Molecular structure of **3** with thermal ellipsoids at the 50% probability level. Hydrogen atoms are omitted for clarity. The ^{i}Pr groups on P atoms are simplified into lines. Selected bond distances (Å): U1–N1 2.73(2), U1–N2 2.260(17), U1–N3 2.739(18), U1–N4 2.37(2), U1–P1 3.15 (3), U1–P2 3.226(12), U1–C1 2.50(2), U1–C2 2.482(17).

metathesis. Treatment of complex **1** with one equivalent of 2,2′-dilithiobiphenyl[62] in THF at RT overnight afforded a brown turbid solution, from which complex **3** was isolated in 76% yield as a yellow crystalline solid (Scheme 2). The ^{1}H NMR spectrum of complex **3** has fourteen peaks between +36.0 and −53.3 ppm, suggesting relatively tight binding of the dimethylamino pendant donor with the U center. The ^{31}P{^{1}H} NMR spectrum of complex **3** showed a single peak at 540.0 ppm, which suggested that the two P atoms are equivalent in solution.

The metallafluorene unit in complex **3** was confirmed by X-ray diffraction (Fig. 4). The two six-membered rings and the five-membered ring of the uranium-containing fluorene unit are co-planar. The bond lengths of U1–C1 (2.50(2) Å) and U1–C2 (2.482(17) Å) are shorter than the U–C_{aryl} bond lengths in $[Li]_2[U(2,3\text{-}C_6H_3CH_2NMe_2)_2(2\text{-}C_6H_4CH_2NMe_2)_2]$ (2.609(4) Å),[51] and $[Li][U(2,3\text{-}C_6H_3CH_2NMe_2)(2\text{-}C_6H_4CH_2NMe_2)_3]$ (2.604(4), 2.650(7), 2.615(8) Å),[53] but are comparable to U–C_{aryl} bond lengths in $[Li(Et_2O)_3][UCl_2(C_6Cl_5)_3]$ (2.497(13), 2.504(13), 2.505 (14) Å).[52] They are also close to those of the U–C_{alkyl} single bond in $[Li(THF)_4][U(CH_2{}^{t}Bu)_5]$ (2.47(1)–2.51(1) Å),[63] $[Li(THF)_4][Li(THF)_2U(CH_3)_6]$ (2.500(5)–2.615(5) Å),[64] UCp* (TMTAA)(CH_2TMTS) (TMTAA = tetramethyl-tetra-aza-annulene) (2.48(1) Å),[65] $[fc(NSi^{t}BuMe_2)_2U(CH_2Ph)(OEt_2)][BPh_4]$ (2.482(12) Å),[47] and $[\eta^5\text{-}1,2,4\text{-}(Me_3C)_3C_5H_2]_2U(\eta^2\text{-}C_4Ph_2)$ (2.448(5)–2.475(5) Å).[66] The bond angle of C1–U1–C2 is 69.1(7)°, which is close to the C–Ln–C angles in $[Li(DME)_3][(C_5Me_5)_2Ln(biphen)]$ (Ln = Ce, 69.0(7)°; Ln = La, 68.55(8)°)[60] but is smaller than the C–M–C angles in other reported metallafluorenes (74°–130°).[56–61,67,68] The bond lengths of U–N_{amine} (average of 2.735 Å) and U–N_{amido} (average of 2.316 Å) are longer than those observed in complex **1** (2.695 and 2.249 Å, respectively), which is probably due to the steric hindrance of the biphenyl group. Complex **3** represents a new example of a heterofluorene containing an actinide element.

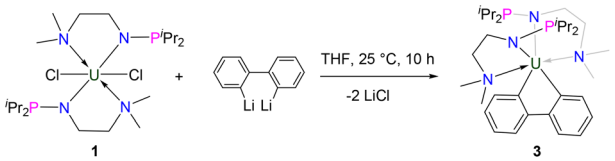

Scheme 2 Synthesis of uranium bi-aryl complex **3**.

We further investigated the reactivity of complex **1** with *o*-$NMe_2C_6H_4CH_2K$ *via* a salt metathesis reaction. Treatment of complex **1** with two equivalents of *o*-$NMe_2C_6H_4CH_2K$ in THF afforded orange crystalline complex **4** in 68% yield (Scheme 3). The ^{1}H NMR spectrum of complex **4** has twenty-nine peaks between +119.3 and −125.1 ppm, which suggested that complex **4** has a low-symmetric structure. The ^{31}P{^{1}H} NMR spectrum of complex **4** was not observed between +1000 and −1000 ppm.

The molecular structure of complex **4** was determined by single-crystal X-ray diffraction, which was revealed to be a unique example of a uranium bi-alkyl metallacycle stabilized by an N-donor (N5) (Fig. 5). The lengths of U–C bonds are 2.461(4) and 2.553(4) Å, which are within the reported range for U–C single bonds (2.29–2.78 Å).[63–66,69–75] The bond lengths of U–N_{amine} (U1–N1 2.734(4) Å, U1–N3 2.813(4) Å, U1–N5 2.568(3) Å) were obviously longer than those of U–N_{amido} (U1–N2 2.297(3) Å, U1–N4 2.285(4) Å), reflecting dative bonding of N1, N3 and N5 to the U center. The bond distances of U1–P1 (3.2145(11) Å) and U1–P2 (3.1286(11) Å) are longer than the sum of the covalent single-bond radii of U and P (2.80 Å), suggesting weak coordination between the two P atoms and the U center.

The sp^3 C–H bond in the dimethylamino moiety of **4** is activated by the uranium centre. This phenomenon was observed previously in actinide organometallic chemistry,[76–78] such as for the formation of uranium hexamethyldisilazide

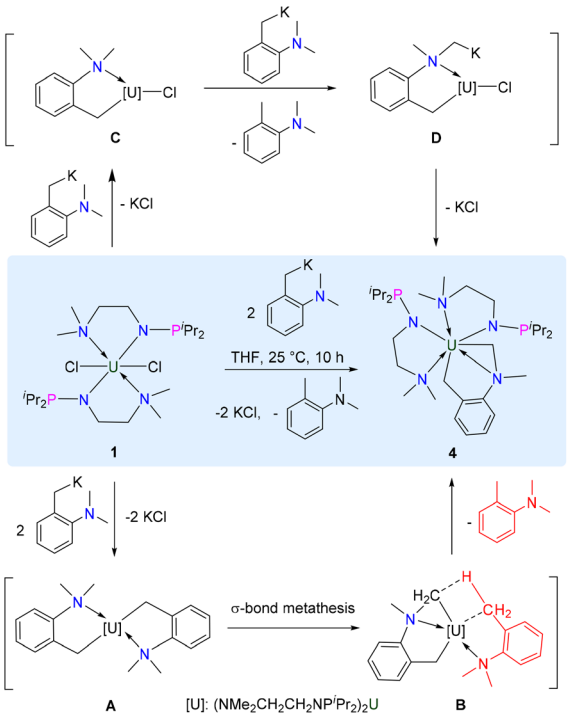

Scheme 3 Synthesis of uranium bi-alkyl complex **4**.

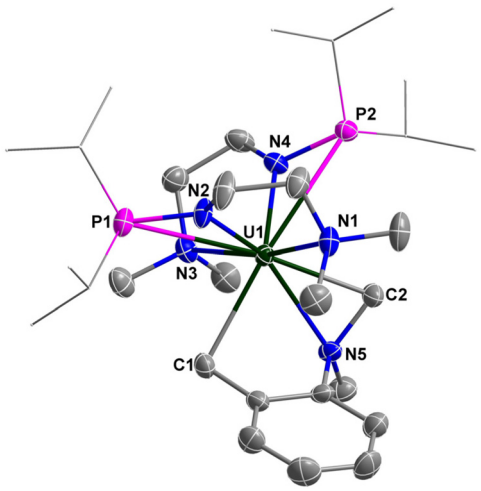

Fig. 5 Molecular structure of **4** with thermal ellipsoids at the 50% probability level. Hydrogen atoms are omitted for clarity. The ^{i}Pr groups on P atoms are simplified into lines. Selected bond distances (Å): U1–N1 2.734(4), U1–N2 2.297(3), U1–N3 2.813(4), U1–N4 2.285(4), U1–N5 2.568(3), U1–P1 3.2145(11), U1–P2 3.1286(11), U1–C1 2.553(4), U1–C2 2.461(4).

metallacles.[79,80] Inspired by the mechanism of generating {[N(CH$_2$CH$_2$NSiMe$_2$^{t}Bu)]$_2$U[η^2-(CH$_2$CH$_2$NSi^{t}Bu(CH$_3$)(CH$_2$))]},[81] two possible routes were proposed for the formation of complex **4** (Scheme 3). Firstly, complex **1** reacts with two equivalents of *o*-NMe$_2$C$_6$H$_4$CH$_2$K to produce intermediate **A** with the release of KCl. Then, the "U-CH$_2$" fragment in intermediate **B** coordinates with the C–H bond in the "NMe$_2$" unit, allowing the σ-bond metathesis to contribute to the production of **4** with the release of *ortho*-dimethylaminotoluene (*o*-NMe$_2$C$_6$H$_5$CH$_3$). On the other hand, complex **1** could react with one equivalent of *o*-NMe$_2$C$_6$H$_4$CH$_2$K to produce intermediate **C**, which could further react with another equivalent of *o*-NMe$_2$C$_6$H$_4$CH$_2$K to produce **D** with the release of *o*-NMe$_2$C$_6$H$_5$CH$_3$. Finally, complex **4** was formed by releasing KCl from intermediate **D**.

The UV-Vis-NIR electronic absorption spectra of **1–4** were measured in THF at RT (Fig. 6). Complexes **1** and **4** showed intense absorption peaks at 216 and 220 nm, respectively. Complexes **2** and **3** showed two absorption peaks at 217 and 233 nm and 214 and 247 nm, respectively. In addition, a weak absorption peak at 420 nm in the visible region was observed for complex **1**. A set of low intensity absorptions were observed in the NIR region for these complexes. For instance, the peaks at 1112 and 1310 nm were found for complex **1**, 1076 and 1305 nm for complex **2**, 1037 and 1294 nm for complex **3**, and 1114 and 1300 nm for complex **4**. These low-intensity absorptions (ε < 150 M^{-1} cm^{-1}) for complexes **1–4** in the NIR region were attributed to the 5f–5f transitions, which are typical features of U(IV) species.

Synthesis of heterometallic clusters 5–7

Clusters with U–M bonds involving transition metals or even main-group metal elements have flourished in recent decades.[82–94] Inspired by our previous isolation of heterometallic clusters with the U–TM bond supported by N–P ligands,[37] we attempted to synthesize heterometallic clusters from complex **1**. Treatment of **1** with one equivalent of RuCl$_2$(PPh$_3$)$_3$ at RT in THF afforded a red-brown solution, from which a crystalline complex **5** was isolated in 42% yield (Scheme 4). Complex **5** is an example of a chlorine-bridged multimetallic cluster with U and Ru. The formal oxidation states of U and Ru in complex **5** are +4 and +2, respectively. The NMR characterization of complex **5** was hindered by the poor solubility of its crystalline species. Attempts to synthesize

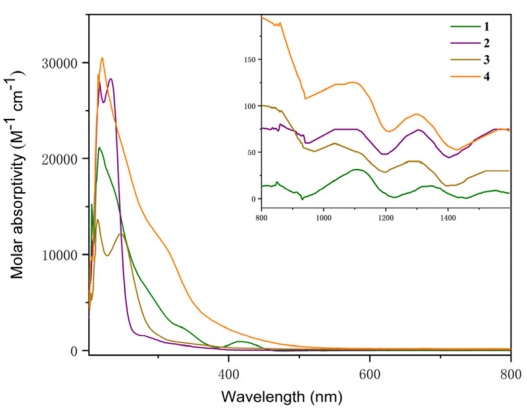

Fig. 6 UV-visible absorption spectra of complexes **1–4** measured in THF at RT (inset: near-infrared absorption spectra).

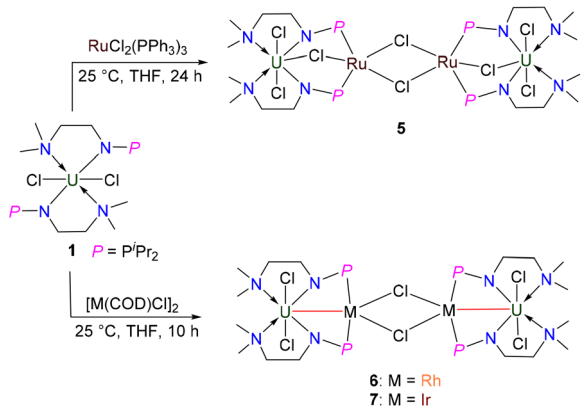

Scheme 4 Synthesis of heterometallic clusters **5**–**7**.

a heterometallic cluster with U–Ru bonds by the reduction of complex **5** with Na, Li, K or KC_8 were unsuccessful.

The solid-state structure of **5** was confirmed by X-ray crystallographic analysis (Fig. 7). The centrosymmetric structure contains a heterometallic U–Ru–Ru–U core with four Cl atom substituents. The bond length of U–Cl3 in the U–Cl–Ru moiety (2.723(2) Å) is longer than the terminal U1–Cl1 (2.707(2) Å) and U1–Cl2 (2.674(3) Å) bond lengths, suggesting the bridged nature of the Cl3 atom. The two P atoms (P1 and P2) are coordinated to the same Ru centre in this species, which is similar to the formation of the U–M bond supported by a dianionic N–P ligand $\{[CH_2O(CH_2)_2NHP^iPr_2]_2\}$.[32] The penta-coordinated Ru centre has an approximately square pyramidal geometry with one of the P atoms at the apical position. The U–Ru distances (3.6349(8) Å) are considerably longer than the sum of the covalent single-bond radii of U and Ru (2.95 Å),[50] suggesting the absence of any bonding interaction between these metal atoms.

To synthesize heterometallic clusters containing U–M bonds, we further attempted the reaction of complex **1** with $[M(COD)Cl]_2$ (M = Rh, Ir). Treatment of **1** with 0.5 equivalents of $[Rh(COD)Cl]_2$ at RT in THF for 10 h afforded complex **6**, which was isolated as a yellow crystalline solid in 57% yield (Scheme 4). Under the same conditions, complex **7** was synthesized by the reaction of complex **1** with 0.5 equivalents of $[Ir(COD)Cl]_2$, and was isolated as a yellow crystalline solid in 45% yield after storing at −30 °C (Scheme 4). Complexes **6** and **7** exhibited extremely low solubility after crystallization and no signals could be observed in the ^{1}H NMR spectra of these clusters even when different deuterated solvents were used.

The molecular structures of **6** and **7** in the solid state were determined by single-crystal X-ray diffraction (Fig. 8 and 9). The crystal systems and space groups of **6** and **7** are monoclinic $P2_1/n$. The coordination environment of the U centers in **6**

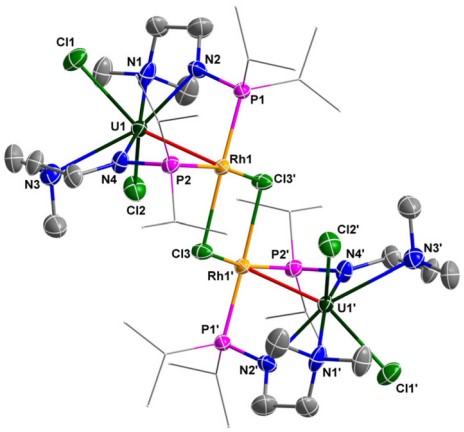

Fig. 8 Molecular structure of **6** with thermal ellipsoids at the 50% probability level. Hydrogen atoms are omitted for clarity. The ^{i}Pr groups on P atoms are simplified into lines. Selected bond distances (Å): U1–N1 2.700(8), U1–N2 2.348(7), U1–N3 2.793(8), U1–N4 2.298(7), U1–Cl1 2.651(2), U1–Cl2 2.696(2), U1–Rh1 2.7910(6), Rh1–Cl3 2.4487(19), Rh1–Cl3′ 2.473(2).

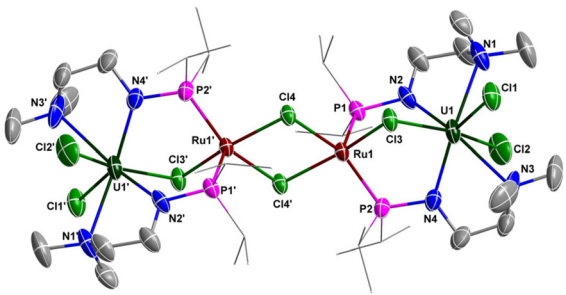

Fig. 7 Molecular structure of **5** with thermal ellipsoids at the 50% probability level. Hydrogen atoms are omitted for clarity. The ^{i}Pr groups on P atoms are simplified into lines. Selected bond distances (Å): U1–N1 2.670(10), U1–N2 2.341(9), U1–N3 2.772(11), U1–N4 2.291(9), U1–Cl1 2.707(2), U1–Cl2 2.674(3), U1–Cl3 2.723(2), Ru1–Cl3 2.3769(19), Ru1–Cl4 2.3899(19), Ru1′–Cl4 2.498(2).

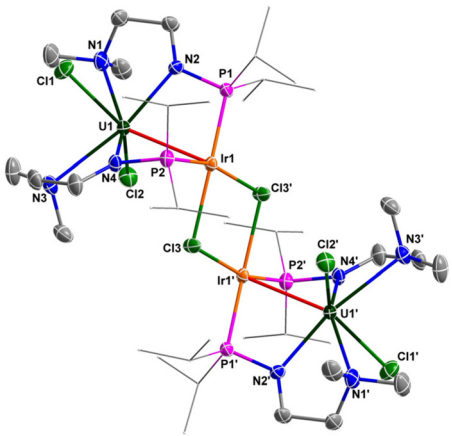

Fig. 9 Molecular structure of **7** with thermal ellipsoids at the 50% probability level. Hydrogen atoms are omitted for clarity. The ^{i}Pr groups on P atoms are simplified into lines. Selected bond distances (Å): U1–N1 2.715(4), U1–N2 2.293(4), U1–N3 2.763(5), U1–N4 2.329(4), U1–Cl1 2.7378(14), U1–Cl2 2.6419(13), U1–Ir1 2.8656(3), Ir1–Cl3 2.4019(12), Ir1–Cl3′ 2.4377(12).

and 7 is very similar, and comprises a hepta-coordinated geometry with one Rh/Ir atom, two Cl atoms, and four N atoms. The Rh and Ir atoms in **6** and **7** adopt almost the same coordination geometry with one U atom, two P atoms, and two Cl atoms. The most remarkable feature of these complexes is the two U–Rh/Ir bonds bridged by two Cl atoms. In complex **6**, the U–Rh bond length is 2.7910(6) Å, which is obviously shorter than the sum of the covalent single-bond radii of U and Rh (2.95 Å).[50] The U–Rh bond length in **6** is longer than the U–Rh single-bond lengths reported in $[U^{IV}I_2(\mu\text{-}OAr^P\text{-}1\kappa^1O,2\kappa^1P)_2Rh^I(\mu\text{-}I)]_2$ (Ar^PO^- = 2-(diphenylphosphino)-6-*tert*-butyl-4-methylphenoxide) (2.7601(5) Å), $U^{IV}I(\mu\text{-}I)(\mu\text{-}OAr^P\text{-}1\kappa^1O,2\kappa^1P)_3Rh^I$ (2.7630(5) Å)[95] and $U[N(CH_3)(CH_2CH_2NP^iPr_2)_2](\mu\text{-}Me)_2Rh_2(\mu\text{-}Me)_4Mg(C_4H_8O)$ (2.6612(5) Å).[34] The U–Ir bond length (2.8656(3) Å) is shorter than the sum of the covalent single-bond radii of U and Ir (2.92 Å), but longer than the U–Ir single-bond length in complex $U[N(CH_3)(CH_2CH_2NP^iPr_2)_2][(\mu\text{-}Me)_2Ir_2(\mu\text{-}Me)_4Mg(C_4H_8O)]$ (2.6968(4) Å).[34] Nevertheless, the U–Rh/Ir bond lengths observed in **6** and **7** are consistent with the presence of a U–M bonding interaction in these clusters.

The UV-Vis-NIR electronic absorption spectra of **5–7** were measured in THF at RT (Fig. 10). Complex **5** exhibited an intense peak at 223 nm and a weak peak at 313 nm in the UV-Vis region. Two peaks at 215 and 326 nm were observed for complex **6** and one intense peak at 219 nm was observed for complex **7**. In the NIR region, complexes **5**, **6** and **7** exhibited similar absorption peaks at 1070 and 1286 nm, 1072 and 1293 nm, and 1067 and 1294 nm, respectively. These weak absorptions (ε < 100 M^{-1} cm^{-1}) were attributed to the f–f transitions expected for U(IV) complexes.

Variable-temperature magnetic data of **5–7** in the solid state were collected using a superconducting quantum interference device (SQUID) (Fig. 11). The effective moments of **5**, **6** and **7** at 300 K are 4.38, 4.77 and 4.54 μ_B per molecule, respectively, which are lower than the theoretical value (5.06 μ_B) for two independent $5f^2$ U(IV) ions. This phenomenon was probably due to the quenching of spin–orbit coupling and was observed for the reported U(IV) complexes.[96] The magnetic moments of

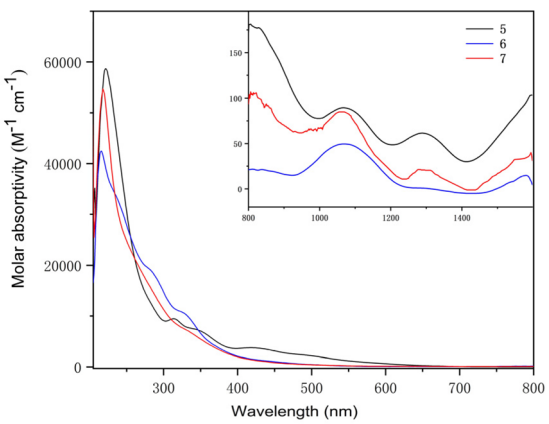

Fig. 10 UV-visible absorption spectra of heterometallic clusters **5–7** measured in THF at RT (inset: near-infrared absorption spectra).

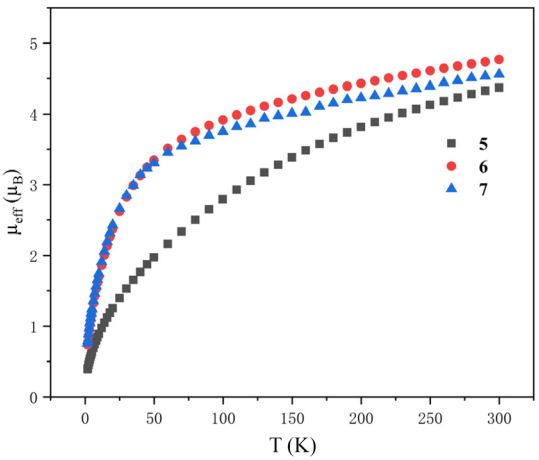

Fig. 11 Variable-temperature effective magnetic moment data. Magnetic moment per molecule for clusters **5–7**.

6 and **7** decline slowly from 300 K to 50 K, and then drop sharply to 0.74 μ_B and 0.76 μ_B at 1.8 K with a trend toward zero. However, the magnetic moment of **5** declines much more obviously and starts to decline from 300 K persistently. At 1.8 K, the magnetic moment of **5** is 0.39 μ_B per molecule. The magnitude of μ_{eff} and temperature dependence of complexes **5**, **6** and **7** are comparable to those observed for the reported U(IV) complexes.

Conclusions

A novel monoanionic N–P ligand **L3** and the corresponding U(IV) complexes **1** and **2** were synthesized. An actinide-containing metallafluorene **3** was synthesized by the reaction of complex **1** and 2,2′-dilithiobiphenyl by a salt metathesis method. Using a similar strategy, U(IV) bi-alkyl complex **4** was isolated by the reaction of complex **1** with *o*-$NMe_2C_6H_4CH_2K$. The monoanionic N–P ligand **L3** also proved to be an effective platform for the construction of heterometallic clusters with U–M bonds. For example, the heterometallic clusters **6** and **7** containing U–Rh or U–Ir bonds were synthesized by the reaction of complex **1** with $[M(COD)Cl]_2$ (M = Rh, Ir). Further studies on the reactivity of the U(IV) bi-aryl complex **3**, the bi-alkyl complex **4** and the heterometallic clusters **5–7** are in progress.

Experimental section

All manipulations were performed under an N_2 atmosphere using standard Schlenk techniques or in an N_2 glovebox (<1 ppm O_2/H_2O). Solvents were dried and deoxygenated by distillation under nitrogen and further dried over 4 Å molecular sieves before use. Benzene-d_6 and THF-d_8 were dried over Na/K and stored under an N_2 atmosphere prior to use. 2,2′-Dilithiobiphenyl,[62] *o*-$NMe_2C_6H_4CH_2K$,[97] UCl_4[98] and

$UI_3(THF)_4$ [44] were prepared using published procedures. Other reagents were purchased and used without further purification. Nuclear magnetic resonance (NMR) spectroscopy was performed using a Bruker AVIII-400 or a Bruker AVIII-500 spectrometer at room temperature (RT). Absolute values of the coupling constants (δ) are provided in Hertz (Hz). Multiplicities of peaks are abbreviated as singlet (s), doublet (d), triplet (t), multiplet (m) or broad (br). Elemental analyses (C, H, N) were performed on a Vario MICRO elemental analyzer at the Center of Modern Analysis of Nanjing University.

Synthesis of L3

A solution of $^{i}Pr_2PCl$ (4.20 g, 27.5 mmol) in THF (10 mL) was added dropwise to a solution of $(CH_3)_2NCH_2CH_2NH_2$ (2.40 g, 27.5 mmol) and Et_3N (15 mL, 110.0 mmol) in THF (20 mL), resulting in the immediate formation of a white precipitate. The mixture was stirred overnight before being dried *in vacuo*. The white solid was extracted with *n*-hexane (20 mL) and then filtered through Celite. Volatiles were removed under reduced pressure to give **L3** as a colorless oil. Yield: 5.00 g (89%). ^{1}H NMR (C_6D_6, 500 MHz, ppm) 2.91–2.95 (m, 2H, NCH_2CH_2), 2.18 (t, $^3J_{HH}$ = 6.1 Hz, 2H, NCH_2CH_2), 2.03 (s, 6H, $N(CH_3)_2$), 1.43–1.52 (m, 2H, $CH(CH_3)_2$), 0.98–1.03 (m, 12H, $CH(CH_3)_2$). $^{13}C\{^1H\}$ NMR (C_6D_6, 125 MHz, ppm) 61.86 (d, J_{PC} = 6.1 Hz, NCH_2CH_2), 46.03 (d, J_{PC} = 23.9 Hz, NCH_2CH_2), 45.07 (s, $N(CH_3)_2$), 26.42 (d, J_{PC} = 13.0 Hz, $CH(CH_3)_2$), 19.10 (d, J_{PC} = 21.0 Hz, $CH(CH_3)_2$), 17.29 (d, J_{PC} = 8.2 Hz, $CH(CH_3)_2$). $^{31}P\{^1H\}$ NMR (C_6D_6, 202 MHz, ppm) 63.68. HRMS (ESI) calcd for $C_{10}H_{26}N_2P$, $[M + H]^+$, m/z = 205.1828. Found 205.1837.

Synthesis of complex 1

Method A. A 2.4 M solution of ^{n}BuLi in *n*-hexane (0.2 mL, 0.5 mmol) was added dropwise to a solution of **L3** (102.2 mg, 0.5 mmol) in THF (4 mL) at −30 °C. The mixture was allowed to warm to RT and stirred for 3 h, and then a solution of UCl_4 (190.0 mg, 0.5 mmol) in THF (5 mL) was added to this mixture. The solution color changed from green to dark green. This solution was stirred at RT for 10 h and then the solvents were removed under reduced pressure. Next, the residues were extracted with toluene (1 mL) and stored at −30 °C overnight to afford green crystalline solid **1** (37.6 mg, 21%).

Method B. A 2.4 M solution of ^{n}BuLi in *n*-hexane (0.8 mL, 2.0 mmol) was added dropwise to a solution of **L3** (408.6 mg, 2.0 mmol) in THF (8 mL) at −30 °C. The mixture was allowed to warm to RT and stirred for 3 h, and then a solution of UCl_4 (380.0 mg, 1.0 mmol) in THF (10 mL) was added to this mixture. The solution color changed from green to dark green. This solution was stirred at RT for 10 h and then the solvents were removed under reduced pressure. Next, the residues were extracted with toluene (3 mL) and the filtrate was dried *in vacuo* and then washed with *n*-hexane (1 mL) to afford complex **1** as a pure green solid (558.1 mg, 78%). Crystals of **1** compatible for X-ray diffraction were grown from a saturated solution in toluene (2 mL) stored at −30 °C. ^{1}H NMR (C_6D_6, 500 MHz, ppm) 54.5 (s, 4H, CH_2), 35.8 (s, 4H, CH_2), 16.5 (s, 14H, $CH(CH_3)_2$), 14.4 (s, 14H, $CH(CH_3)_2$), −70.5 (s, 12H, $N(CH_3)_2$). $^{31}P\{^1H\}$ NMR (C_6D_6, 162 MHz, ppm) was not observed in the range of +1000 to −1000 ppm. Anal. calcd (%) for $C_{20}H_{48}Cl_2N_4P_2U$: C, 33.57; H, 6.76; N, 7.83. Found: C, 33.82; H, 6.71; N, 7.79.

Synthesis of complex 2

Method A. A 2.4 M solution of ^{n}BuLi in *n*-hexane (0.4 mL, 1.0 mmol) was added dropwise to a solution of **L3** (204.3 mg, 1.0 mmol) in THF (4 mL) at −30 °C. The mixture was stirred for 3 h, and was then added to a solution of $UI_3(THF)_4$ (2/3 equiv., 602.1 mg, 0.7 mmol) in THF (5 mL). The mixture was stirred at RT for 10 h and then the solvents were removed under reduced pressure. Next, the residues were extracted with toluene (1 mL) and the filtrate was stored at −30 °C to afford complex **2** as red-orange crystals (166.2 mg, 37% based on ligand).

Method B. Trimethylsilyl iodide (80.0 mg, 0.4 mmol) dissolved in toluene (0.5 mL) was added to a solution of complex **1** (143.1 mg, 0.2 mmol) in toluene (2 mL). The solution immediately changed from green to red-orange. The mixture was stirred at RT for 6 h and then the solvents were removed under reduced pressure to afford complex **2** as a pure red-orange solid without subsequent purification. Yield: **2** (163.5 mg, 91%). Crystals of **2** compatible for X-ray diffraction were grown from a saturated solution in toluene (1 mL) stored at −30 °C. ^{1}H NMR (C_6D_6, 400 MHz, ppm) 58.0 (s, 4H, CH_2), 35.1 (s, 4H, CH_2), 24.3 (s, 14H, $CH(CH_3)_2$), 12.8 (s, 14H, $CH(CH_3)_2$), −74.4 (s, 12H, $N(CH_3)_2$). $^{31}P\{^1H\}$ NMR (C_6D_6, 162 MHz, ppm) was not observed in the range of +1000 to −1000 ppm. Anal. calcd (%) for $C_{20}H_{48}I_2N_4P_2U$: C, 26.74; H, 5.39; N, 6.24. Found: C, 26.61; H, 5.49; N, 6.38.

Synthesis of complex 3

Complex **1** (143.1 mg, 0.2 mmol) and 2,2′-dilithiobiphenyl (33.2 mg, 0.2 mmol) were added to a 5 mL flask and dissolved in THF (2 mL). The solution immediately changed from green to red-orange. The mixture was stirred at RT for 10 h and then the solvent was removed under reduced pressure and the residue was extracted with ether (3 mL). The filtrate was dried *in vacuo* to afford complex **3** as a pure yellow solid (121.1 mg, 76%). Crystals of **3** compatible for X-ray diffraction were grown from a saturated solution in ether (2 mL) stored at RT. ^{1}H NMR (C_6D_6, 400 MHz, ppm) 36.0 (d, J = 18.7 Hz, 4H, CH_2), 26.6 (d, J = 8.7 Hz, 2H, $CH(CH_3)_2$), 25.8 (d, J = 34.1 Hz, 4H, CH_2), 21.3 (s, 2H, biphenyl), 17.5 (t, J = 6.5 Hz, 2H, $CH(CH_3)_2$), 15.7 (s, 2H, biphenyl), 13.0 (s, 6H, $CH(CH_3)_2$), 9.4 (s, 6H, $CH(CH_3)_2$), 8.9 (s, 6H, $CH(CH_3)_2$), 6.8 (s, 6H, $CH(CH_3)_2$), −24.5 (s, 2H, biphenyl), −26.0 (s, 6H, $N(CH_3)_2$), −43.7 (s, 2H, biphenyl), −53.3 (s, 6H, $N(CH_3)_2$). $^{31}P\{^1H\}$ NMR (C_6D_6, 162 MHz, ppm) 540.0. Anal. calcd (%) for $C_{32}H_{56}N_4P_2U$: C, 48.24; H, 7.08; N, 7.03. Found: C, 47.01; H, 6.91; N, 6.87. No satisfactory result for the C% value was obtained despite repeated attempts, which is probably due to the inadequate combustion of this air- and moisture-sensitive species.

Synthesis of complex 4

Complex **1** (71.5 mg, 0.1 mmol) and *o*-$NMe_2C_6H_4CH_2K$ (34.7 mg, 0.2 mmol) were added to a 5 mL flask and dissolved in THF (2 mL). The solution immediately changed from green to orange. The mixture was stirred at RT overnight. Then the solvent was removed under reduced pressure and the residue was extracted with *n*-hexane (3 mL). Yellow crystals of **4** were grown from a solution of ether (2 mL) at room temperature. Yield: **4** (52.9 mg, 68%). ^{1}H NMR (d_8-THF, 400 MHz, ppm) 119.3 (s, 1H), 98.4 (s, 1H), 95.2 (s, 3H), 88.7 (s, 1H), 67.4 (s, 1H), 48.5 (s, 1H), 43.5 (s, 3H), 38.9 (s, 3H), 31.4 (s, 4H), 23.2 (s, 4H), 20.8 (s, 1H), 8.2 (s, 3H), −1.3 (s, 2H), −1.9 (s, 3H), −6.9 (s, 3H), −12.5 (s, 1H), −16.8 (s, 4H), −28.4 (s, 1H), −30.7 (s, 1H), −34.5 (s, 1H), −41.1 (s, 1H), −45.8 (s, 3H), −48.0 (s, 1H), −50.8 (s, 1H), −63.2 (s, 3H), −67.4 (s, 3H), −74.1 (s, 1H), −96.2 (s, 3H), −125.1 (s, 1H). ^{31}P{^{1}H} NMR (C_6D_6, 162 MHz, ppm) was not observed in the range of +1000 to −1000 ppm. Anal. calcd (%) for $C_{29}H_{59}N_5P_2U$: C, 44.78; H, 7.65; N, 9.00. Found: C, 44.70; H, 7.55; N, 8.91.

Synthesis of complex 5

A solution of $RuCl_2(PPh_3)_3$ (95.9 mg, 0.1 mmol) in THF (2 mL) was added to a solution of complex **1** (71.5 mg, 0.1 mmol) in THF (2 mL) at RT. The mixture was left undisturbed for 1 day at RT. Then, black block crystals of **5** (74.6 mg, 42%) were obtained. NMR characterization of this species was prevented by its poor solubility after recrystallization. Anal. calcd (%) for $C_{40}H_{96}Cl_8N_8P_4Ru_2U_2{\cdot}2C_4H_8O$: C, 30.04; H, 5.88; N, 5.84. Found: C, 30.27; H, 5.65; N, 5.97.

Synthesis of complex 6

A solution of $[Rh(COD)Cl]_2$ (33.7 mg, 0.1 mmol) in THF (2 mL) was added to a solution of complex **1** (143.1 mg, 0.2 mmol) in THF (2 mL) at RT. The solution immediately changed from green to orange. The mixture was stirred at RT overnight and then the solvents were removed. The residue was extracted with dichloromethane (2 mL). Storing the filtrate at −30 °C for 18 h yielded product **6** as orange block crystals (97.3 mg, 57%). NMR characterization of this species was prevented by its poor solubility after recrystallization. Anal. calcd (%) for $C_{40}H_{96}Cl_6N_8P_4Rh_2U_2$: C, 28.13; H, 5.67; N, 6.56. Found: C, 28.34; H, 5.73; N, 6.44.

Synthesis of complex 7

A solution of $[Ir(COD)Cl]_2$ (51.5 mg, 0.1 mmol) in THF (2 mL) was added to a solution of complex **1** (143.1 mg, 0.2 mmol) in THF (3 mL). The color of the solution immediately changed from green to orange. The mixture was stirred at RT overnight and then the solvents were removed. The residue was extracted with dichloromethane (2 mL). Storing the filtrate at −30 °C for 24 h yielded product **7** as orange block crystals (84.9 mg, 45%). NMR characterization of this species was prevented by its poor solubility after recrystallization. Anal. calcd (%) for $C_{40}H_{96}Cl_6N_8P_4Ir_2U_2$: C, 25.47; H, 5.13; N, 5.94. Found: C, 25.76; H, 5.14; N, 5.87.

Single-crystal X-ray diffraction

The crystallographic data of complexes **1**, **2**, **3**, **4**, **5**, **6** and **7** were collected on Bruker D8 venture photon II detectors at 193 K or 296 K with a radiation source of Ga(Kα) (λ = 1.34139 Å) or Mo(Kα) (λ = 0.71073 Å) using the ω-scan technique. Multiscan or empirical absorption corrections (SADABS) were applied.[99] The structures were solved by direct methods, expanded by difference Fourier syntheses, and refined by full-matrix least squares on F^2 using Olex2.[100] All non-hydrogen atoms were refined on F^2 by full-matrix least-squares procedures with the use of anisotropic displacement parameters.[101] Hydrogen atoms were introduced at their geometric positions and refined as riding atoms. In complex **3**, the "$CH_2NP^iPr_2$" unit was split into two parts with 43.3% and 56.7% occupancies. The X-ray crystal structures have been deposited in the Cambridge Crystallographic Data Centre (CCDC 2254129 (**1**), 2254126 (**2**), 2254132 (**3**), 2254127 (**4**), 2254131 (**5**), 2254128 (**6**), and 2254130 (**7**)†). Details of the data collection and refinement for complexes **1**, **2**, **3**, **4**, **5**, **6** and **7** are given in Tables S1, S2 and S3 in the ESI.†

Author contributions

Kai Li: investigation, writing – original draft. Jialu He: investigation. Yue Zhao: software. Congqing Zhu: resources, supervision, funding acquisition, writing – review & editing.

Conflicts of interest

The authors declare no conflict of interest.

Acknowledgements

This research was supported by the National Key R&D Program of China (2021YFA1502500), the National Natural Science Foundation of China (No. 91961116 and 22271138), and the Natural Science Foundation of Jiangsu Province (BK20220065), Programs for High-Level Entrepreneurial and Innovative Talents Introduction of Jiangsu Province.

References

1 T. Storr, *Ligand design in medicinal inorganic chemistry*, John Wiley & Sons, 2014.
2 M. Stradiotto, *Ligand design in metal chemistry: reactivity and catalysis*, John Wiley & Sons, 2016.
3 T. J. Kealy and P. L. Pauson, A new type of organo-iron compound, *Nature*, 1951, **168**, 1039–1040.
4 L. T. Reynolds and G. Wilkinson, π-cyclopentadienyl compounds of uranium-IV and thorium-IV, *J. Inorg. Nucl. Chem.*, 1956, **2**, 246–253.

5 G. I. Vargas-Zuniga, M. A. Boreen, D. N. Mangel, J. Arnold and J. L. Sessler, Porphyrinoid actinide complexes, *Chem. Soc. Rev.*, 2022, **51**, 3735–3758.
6 K. Li, W. Liu, H. Zhang, L. Cheng, Y. Zhang, Y. Wang, N. Chen, C. Zhu, Z. Chai and S. Wang, Progress in solid state and coordination chemistry of actinides in China, *Radiochim. Acta*, 2023, **111**(1), 1–42.
7 Y. Wang, S. Hu, L. Cheng, C. Liang, X. Yin, H. Zhang, A. Li, D. Sheng, J. Diwu, X. Wang, J. Li, Z. Chai and S. Wang, Stabilization of plutonium(v) within a crown ether inclusion complex, *CCS Chem.*, 2020, **2**, 425–431.
8 Q. Liu and L. Zhao, Low valent palladium clusters: synthesis, structures and catalytic applications, *Chin. J. Chem.*, 2020, **38**, 1897–1908.
9 Y. Liu, L. Cui, W. Fang and J. Zhang, Design and synthesis of Al_7Ni_2 heterometallic clusters based on metal substitution and ligands protection strategies, *Chin. J. Chem.*, 2023, **41**, 521–526.
10 W. Fang, S. Pan, W. Su, S. Wang, L. Zhao, G. Frenking and C. Zhu, Complex featuring two double dative bonds between carbon(0) and uranium, *CCS Chem.*, 2022, **4**, 1921–1929.
11 W. Su, S. Pan, X. Sun, S. Wang, L. Zhao, G. Frenking and C. Zhu, Double dative bond between divalent carbon(0) and uranium, *Nat. Commun.*, 2018, **9**, 4997.
12 M. Falcone, L. Barluzzi, J. Andrez, F. F. Tirani, I. Živković, A. Fabrizio, C. Corminboeuf, K. Severin and M. Mazzanti, The role of bridging ligands in dinitrogen reduction and functionalization by uranium multimetallic complexes, *Nat. Chem.*, 2019, **11**, 154–160.
13 M. Falcone, L. Chatelain, R. Scopelliti, I. Živković and M. Mazzanti, Nitrogen reduction and functionalization by a multimetallic uranium nitride complex, *Nature*, 2017, **547**, 332–335.
14 C. D. Tutson and A. E. V. Gorden, Thorium coordination: A comprehensive review based on coordination number, *Coord. Chem. Rev.*, 2017, **333**, 27–43.
15 S. T. Liddle, The renaissance of non-aqueous uranium chemistry, *Angew. Chem., Int. Ed.*, 2015, **54**, 8604–8641.
16 M. Ephritikhine, Recent advances in organoactinide chemistry as exemplified by cyclopentadienyl compounds, *Organometallics*, 2013, **32**, 2464–2488.
17 J. L. Sessler, P. J. Melfi and G. D. Pantos, Uranium complexes of multidentate N-donor ligands, *Coord. Chem. Rev.*, 2006, **250**, 816–843.
18 J. Yu, K. Liu, Q. Wu, B. Li, X. Kong, K. Hu, L. Mei, L. Yuan, Z. Chai and W. Shi, Facile access to uranium and thorium phosphaethynolate complexes supported by tren: experimental and theoretical study, *Chin. J. Chem.*, 2021, **39**, 2125–2131.
19 P. B. Hitchcock and P. Scott, Synthesis of tripodal amido complexes of the early actinides; molecular structure of $\{N[CH_2CH_2N(SiMe_3)]_3UCl\}_2$, *Polyhedron*, 1994, **13**, 1651–1653.
20 W. Su, T. Rajeshkumar, L. Xiang, L. Maron and Q. Ye, Facile synthesis of uranium complexes with a pendant borane lewis acid and 1,2-insertion of CO into a U-N bond, *Angew. Chem., Int. Ed.*, 2022, **61**, e202212823.
21 Q. Wu, C. Wang, J. Lan, Z. Chai and W. Shi, Electronic structures and bonding of the actinide halides An $(TREN^{TIPS})X$ (An=Th-Pu; X=F-I): a theoretical perspective, *Dalton Trans.*, 2020, **49**, 15895–15902.
22 K. Liu, J. Yu, Q. Wu, X. Tao, X. Kong, L. Mei, K. Hu, L. Yuan, Z. Chai and W. Shi, Rational design of a tripodal ligand for U(iv): synthesis and characterization of a U-Cl species and insights into its reactivity, *Organometallics*, 2020, **39**, 4069–4077.
23 J. T. Boronski, J. A. Seed, D. Hunger, A. W. Woodward, J. Slageren, A. J. Wooles, L. S. Natrajan, N. Kaltsoyannis and S. T. Liddle, A crystalline tri-thorium cluster with σ-aromatic metal-metal bonding, *Nature*, 2021, **598**, 72–75.
24 B. M. Gardner, C. E. Kefalidis, E. Lu, D. Patel, E. J. L. Mclnnes, F. Tuna, A. J. Wooles, L. Maron and S. T. Liddle, Evidence for single metal two electron oxidative addition and reductive elimination at uranium, *Nat. Commun.*, 2017, **8**, 1898.
25 D. M. King, F. Tuna, E. J. L. Mclnnes, J. McMaster, W. Lewis, A. J. Blake and S. T. Liddle, Synthesis and structure of a terminal uranium nitride complex, *Science*, 2012, **337**, 717–720.
26 D. M. King, F. Tuna, E. J. L. Mclnnes, J. McMaster, W. Lewis, A. J. Blake and S. T. Liddle, Isolation and characterization of a uranium(vi)-nitride triple bond, *Nat. Chem.*, 2013, **5**, 482–488.
27 P. Roussel and P. Scott, Complex of dinitrogen with trivalent uranium, *J. Am. Chem. Soc.*, 1998, **120**, 1070–1071.
28 S. C. Bart, C. Anthon, F. W. Heinemann, E. Bill, N. M. Edelstein and K. Meyer, Carbon dioxide activation with sterically pressured mid- and high-valent uranium complexes, *J. Am. Chem. Soc.*, 2008, **130**, 12536–12546.
29 G. Feng, M. Zhang, D. Shao, X. Wang, S. Wang, L. Maron and C. Zhu, Transition-metal-bridged bimetallic clusters with multiple uranium-metal bonds, *Nat. Chem.*, 2019, **11**, 248–253.
30 G. Feng, M. Zhang, P. Wang, S. Wang, L. Maron and C. Zhu, Identification of a uranium-rhodium triple bond in a heterometallic cluster, *Proc. Natl. Acad. Sci. U. S. A.*, 2019, **116**, 17654–17658.
31 P. Wang, I. Douair, Y. Zhao, R. Ge, J. Wang, S. Wang, L. Maron and C. Zhu, Selective hydroboration of terminal alkynes catalyzed by heterometallic clusters with uranium-metal triple bonds, *Chem*, 2022, **8**, 1361–1375.
32 G. Feng, K. McCabe, S. Wang, L. Maron and C. Zhu, Construction of heterometallic clusters with multiple uranium-metal bonds by using dianionic nitrogen-phosphorus ligands, *Chem. Sci.*, 2020, **11**, 7585–7592.
33 X. Xin, I. Douair, Y. Zhao, S. Wang, L. Maron and C. Zhu, Dinitrogen cleavage by a heterometallic cluster featuring multiple uranium-rhodium bonds, *J. Am. Chem. Soc.*, 2020, **142**, 15004–15011.
34 J. Shen, T. Rajeshkumar, G. Feng, Y. Zhao, S. Wang, L. Maron and C. Zhu, Complexes featuring a cis-

[M⇉U⇇M] core (M=Rh, Ir): a new route to uranium-metal multiple bonds, *Angew. Chem., Int. Ed.*, 2023, **62**, e202303379.

35 L. Barluzzi, S. R. Giblin, A. Mansikkamaki and R. A. Layfield, Identification of oxidation state +1 in a molecular uranium complex, *J. Am. Chem. Soc.*, 2022, **144**, 18229–18233.

36 R. A. K. Shivaraam, M. Keener, D. K. Modder, T. Rajeshkumar, I. Živković, R. Scopelliti, L. Maron and M. Mazzanti, A route to stabilize uranium(II) and uranium (I) synthons in multimetallic complexes, *Angew. Chem., Int. Ed.*, 2023, **62**, e202304051.

37 Q. Zhu, W. Fang, L. Maron and C. Zhu, Heterometallic clusters with uranium-metal bonds supported by double-layer nitrogen-phosphorus ligands, *Acc. Chem. Res.*, 2022, **55**, 1718–1730.

38 X. Xin, I. Douair, Y. Zhao, S. Wang, L. Maron and C. Zhu, Dinitrogen cleavage and hydrogenation to ammonia with a uranium complex, *Natl. Sci. Rev.*, 2023, **10**, nwac144.

39 X. Xin, I. Douair, T. Rajeshkumar, Y. Zhao, S. Wang, L. Maron and C. Zhu, Photochemical synthesis of transition metal-stabilized uranium(VI) nitride complexes, *Nat. Commun.*, 2022, **13**, 3809.

40 P. Wang, Y. Zhao and C. Zhu, Photolysis, thermolysis, and reduction of a uranium azide complex supported by a double-layer N-P ligand, *Organometallics*, 2022, **41**, 2448–2454.

41 X. Sun, X. Gong, Z. Xie and C. Zhu, A uranium(IV) alkyl complex: synthesis and catalytic property in carbonyl hydroboration, *Chin. J. Chem.*, 2022, **40**, 2047–2053.

42 P. Wang, I. Douair, Y. Zhao, S. Wang, J. Zhu, L. Maron and C. Zhu, Facile dinitrogen and dioxygen cleavage by a uranium(III) complex: cooperativity between the non-innocent ligand and the uranium center, *Angew. Chem., Int. Ed.*, 2021, **60**, 473–479.

43 W. Fang, I. Douair, A. Hauser, K. Li, Y. Zhao, P. W. Roesky, S. Wang, L. Maron and C. Zhu, Uranium(III)-phosphorus (III) synergistic activation of white phosphorus and arsenic, *CCS Chem.*, 2022, **4**, 2630–2638.

44 T. V. Fetrow, J. P. Grabow, J. Leddy and S. R. Daly, Convenient syntheses of trivalent uranium halide starting materials without uranium metal, *Inorg. Chem.*, 2021, **60**, 7593–7601.

45 A. L. Odom, P. L. Arnold and C. C. Cummins, Heterodinuclear Uranium/molybdenum dinitrogen complexes, *J. Am. Chem. Soc.*, 1998, **120**, 5836–5837.

46 P. L. Diaconescu and C. C. Cummins, Diuranium inverted sandwiches involving naphthalene and cyclooctatetraene, *J. Am. Chem. Soc.*, 2002, **124**, 7660–7661.

47 M. J. Monreal and P. L. Diaconescu, A weak interaction between iron and uranium in uranium alkyl complexes supported by ferrocene diamide ligands, *Organometallics*, 2008, **27**, 1702–1706.

48 S. Duhović, S. Khan and P. L. Diaconescu, In situ generation of uranium alkyl complexes, *Chem. Commun.*, 2010, **46**, 3390–3392.

49 J. W. Napoline, S. J. Kraft, E. M. Matson, P. E. Fanwick, S. C. Bart and C. M. Thomas, Tris(phosphinoamide)-supported uranium-cobalt heterobimetallic complexes featuring Co→U dative interactions, *Inorg. Chem.*, 2013, **52**, 12170–12177.

50 P. Pyykko, Additive covalent radii for single, double, and triple-bonded molecules and tetrahedrally bonded crystals: a summary, *J. Phys. Chem. A*, 2015, **119**, 2326–2337.

51 E. A. Pedrick, L. A. Seaman, J. C. Scott, L. Griego, G. Wu and T. W. Hayton, Synthesis and reactivity of a U(IV) dibenzyne complex, *Organometallics*, 2016, **35**, 494–502.

52 O. Ordonez, X. Yu, G. Wu, J. Autschbach and T. W. Hayton, Homoleptic perchlorophenyl "ate" complexes of thorium(IV) and uranium(IV), *Inorg. Chem.*, 2021, **60**, 12436–12444.

53 L. A. Seaman, E. A. Pedrick, T. Tsuchiya, G. Wu, E. Jakubikova and T. W. Hayton, Comparison of the reactivity of 2-Li-$C_6H_4CH_2NMe_2$ with MCl_4 (M=Th, U): isolation of a thorium aryl complex or a uranium benzyne complex, *Angew. Chem., Int. Ed.*, 2013, **52**, 10589–10592.

54 S. Fortier, B. C. Melot, G. Wu and T. W. Hayton, Homoleptic uranium(IV) alkyl complexes: synthesis and characterization, *J. Am. Chem. Soc.*, 2009, **131**, 15512–15521.

55 M. A. Boreen, B. F. Parker, T. D. Lohrey and J. Arnold, A homoleptic uranium(III) tris(aryl) complex, *J. Am. Chem. Soc.*, 2016, **138**, 15865–15868.

56 T. Delouche, M. Hissler and P. Bouit, Polycyclic aromatic hydrocarbons containing heavy group 14 elements: from synthetic challenges to optoelectronic devices, *Coord. Chem. Rev.*, 2022, **464**, 214553.

57 X. Su, T. A. Bartholome, J. R. Tidwell, A. Pujol, S. Yruegas, J. J. Martinez and C. D. Martin, 9-Borafluorenes: synthesis, properties, and reactivity, *Chem. Rev.*, 2021, **121**, 4147–4192.

58 W. Ma, C. Yu, T. Chen, L. Xu, W.-X. Zhang and Z. Xi, Metallacyclopentadienes: synthesis, structure and reactivity, *Chem. Soc. Rev.*, 2017, **46**, 1160–1192.

59 A. Steffen, R. M. Ward, W. D. Jones and T. B. Marder, Dibenzometallacyclopentadienes, boroles and selected transition metal and main group heterocyclopentadienes: synthesis, catalytic and optical properties, *Coord. Chem. Rev.*, 2010, **254**, 1950–1976.

60 P. Pandey, X. Yu, G. B. Panetti, E. Lapsheva, M. R. Gau, P. J. Carroll, J. Autschbach and E. J. Schelter, Synthesis, electrochemical, and computational studies of organocerium(III) complexes with Ce-aryl sigma bonds, *Organometallics*, 2023, **42**, 1267–1277.

61 M. Zhu, Z. Chai, Z.-J. Lv, T. Liu, W. Liu, J. Wei and W.-X. Zhang, Selective cleavage of the strong or weak C-C bonds in biphenylene enabled by rare-earth metals, *J. Am. Chem. Soc.*, 2023, **145**, 6633–6638.

62 Z. Huang, Y. Zhang, W.-X. Zhang, J. Wei, S. Ye and Z. Xi, A tris-spiro metalla-aromatic system featuring Craig-Möbius aromaticity, *Nat. Commun.*, 2021, **12**, 1319.

63 S. Fortier, B. Melot, G. Wu and T. W. Hayton, Homoleptic uranium(IV) alkyl complexes: synthesis and characterization, *J. Am. Chem. Soc.*, 2009, **131**, 15512–15521.
64 J. D. Sears, D. Sergentu, T. M. Baker, W. W. Brennessel, J. Autschbach and M. L. Neidig, The exceptional diversity of homoleptic uranium-methyl complexes, *Angew. Chem., Int. Ed.*, 2020, **59**, 13586–13590.
65 S. Hohloch, M. E. Garner, B. F. Parker and J. Arnold, New supporting ligands in actinide chemistry: tetramethyltetraazaannulene complexes with thorium and uranium, *Dalton Trans.*, 2017, **46**, 13768–13782.
66 D. Wang, W. Ding, G. Hou, G. Zi and M. D. Walter, Uranium versus thorium: synthesis and reactivity of $[\eta^5$-1,2,4$(Me_3C)_3C_5H_2]_2U[\eta^2$-$C_2Ph_2]$, *Chem. – Eur. J.*, 2021, **27**, 6767–6782.
67 Y. Du, Y. Xiao, F. Tian, L. Han, Y. Gu and N. Zhu, Progress in annulative transformation from indoles to carbazoles: state of the art, *Chin. J. Org. Chem.*, 2021, **41**, 521–528.
68 W. Cao and X. Liu, Electrochemical 1,2-diarylation of alkenes enabled by direct dual C-H functionalization of elextron-rich aromatic hydrocarbons, *Chin. J. Org. Chem.*, 2021, **41**, 857–858.
69 P. L. Diaconescu, Reactions of aromatic N-heterocycles with d^0f^n-metal alkyl complexes supported by chelating diamide ligands, *Acc. Chem. Res.*, 2010, **43**, 1352–1363.
70 N. R. Andreychuk, S. Lango, B. Vidjayacoumar, D. J. Emslie and H. A. Jenkins, Uranium(IV) alkyl complexes of a rigid dianionic NON-donor ligand: synthesis and quantitative alkyl exchange reactions with alkyllithium reagents, *Organometallics*, 2013, **32**, 1466–1474.
71 S. A. Johnson and S. C. Bart, Achievements in uranium alkyl chemistry: celebrating sixty years of synthetic pursuits, *Dalton Trans.*, 2015, **44**, 7710–7726.
72 L. Zhang, G. Hou, G. Zi, W. Ding and M. D. Walter, Influence of the 5f orbitals on the bonding and reactivity in organoactinides: experimental and computational studies on a uranium metallacyclopropene, *J. Am. Chem. Soc.*, 2016, **138**, 5130–5142.
73 L. Zhang, B. Fang, G. Hou, G. Zi, W. Ding and M. D. Walter, Experimental and computational studies of a uranium metallacyclocumulene, *Organometallics*, 2017, **36**, 898–910.
74 G. Zi, Recent developments in actinide metallacycles, *Chem. Commun.*, 2018, **54**, 7412–7430.
75 S. A. Johnson, R. F. Higgins, M. M. Abu-Omar, M. P. Shores and S. C. Bart, Mechanistic insights into concerted C-C reductive elimination from homoleptic uranium alkyls, *Organometallics*, 2017, **36**, 3491–3497.
76 J. A. Pool, B. L. Scott and J. L. Kiplinger, A new mode of reactivity for pyridine N-oxide: C-H activation with uranium(IV) and thorium(IV) bis(alkyl) complexes, *J. Am. Chem. Soc.*, 2005, **127**, 1338–1339.
77 W. Evans, J. Walensky and J. Ziller, Synthesis of a thorium tuck-in complex, $[(\eta^5{:}\eta^1$-$C_5Me_4CH_2)$ $(\eta^5$-$C_5Me_5)Th\{^iPrNC(Me)N^iPr\}]$, by C-H bond activation initiated by $(C_5Me_5)^-$, *Chem. – Eur. J.*, 2009, **15**, 12204–12207.
78 B. M. Gardner, P. A. Cleaves, C. E. Kefalidis, J. Fang, L. Maron, W. Lewis, A. J. Blake and S. T. Liddle, The role of 5f-orbital participation in unexpected inversion of the σ-bond metathesis reactivity trend of triamidoamine thorium(IV) and uranium(IV) alkyls, *Chem. Sci.*, 2014, **5**, 2489–2497.
79 J. M. Berg, D. L. Clark, J. C. Huffman, D. E. Morris, A. P. Sattelberger, W. E. Streib, W. G. Van Der Sluys and J. G. Watkin, Early actinide alkoxide chemistry. synthesis, characterization, and molecular structures of Th(IV) and U(IV) aryloxide complexes, *J. Am. Chem. Soc.*, 1992, **114**, 10811–10821.
80 M. J. Monreal, R. K. Thomson, T. Cantat, N. E. Travia, B. L. Scott and J. L. Kiplinger, UI_4(1,4-dioxane)$_2$, $[UCl_4$(1,4-dioxane)$]_2$, and UI_3(1,4-dioxane)$_{1.5}$: stable and versatile starting materials for low- and high-valent uranium chemistry, *Organometallics*, 2011, **30**, 2031–2038.
81 R. Boaretto, P. Roussel, N. W. Alcock, A. J. Kingsley, I. J. Munslow, C. J. Sanders and P. Scott, Synthesis of a highly strained uranacycle: molecular structures of organometallic products arising from reduction, oxidation and protonolysis, *J. Organomet. Chem.*, 1999, **591**, 174–184.
82 R. S. Sternal and T. J. Marks, Actinide-to-transition metal bonds. synthesis, characterization, and properties of metal-metal bonded systems having the tris(cyclopentadlenyl)actinide fragment, *Organometallics*, 1987, **6**, 2621–2623.
83 S. G. Minasian, J. L. Krinsky, V. A. Williams and J. Arnold, A heterobimetallic complex with an unsupported uranium (III)-aluminum(I) bond: $(CpSiMe_3)_3U$-$AlCp^*$ (Cp^*=C_5Me_5), *J. Am. Chem. Soc.*, 2008, **130**, 10086–10087.
84 S. G. Minasian, J. Krinsky, J. D. Rinehart, R. Copping, T. Tyliszczak, M. Janousch, D. K. Shuh and J. Arnold, A comparison of 4f *vs* 5f metal-metal bonds in $(CpSiMe_3)_3$M-ECp^* (M=Nd, U; E=Al, Ga; Cp*=C_5Me_5): synthesis, thermodynamics, magnetism, and electronic structure, *J. Am. Chem. Soc.*, 2009, **131**, 13767–13783.
85 S. T. Liddle, J. McMaster, D. P. Mills, A. J. Blake, C. Jones and W. D. Woodul, σ and π donation in an unsupported uranium-gallium bond, *Angew. Chem., Int. Ed.*, 2009, **48**, 1077–1080.
86 S. T. Liddle and D. P. Mills, Metal-metal bonds in f-element chemistry, *Dalton Trans.*, 2009, 5592–5605.
87 S. T. Liddle, Non-traditional ligands in f-block chemistry, *Proc. R. Soc. A*, 2009, **465**, 1673–1700.
88 D. Patel, F. Moro, J. McMaster, W. Lewis, A. J. Blake and S. T. Liddle, A formal high oxidation state inverse-sandwich diuranium complex: a new route to f-block-metal bonds, *Angew. Chem., Int. Ed.*, 2011, **50**, 10388–10392.
89 B. Oelkers, M. V. Butovskii and R. Kempe, F-element-metal bonding and the use of the bond polarity to build molecular intermetalloids, *Chem. – Eur. J.*, 2012, **18**, 13566–13579.
90 A. L. Ward, W. W. Lukens, C. C. Lu and J. Arnold, Photochemical route to actinide-transition metal bonds:

synthesis, characterization and reactivity of a series of thorium and uranium heterobimetallic complexes, *J. Am. Chem. Soc.*, 2014, **136**, 3647–3654.

91 J. A. Hlina, J. R. Pankhurst, N. Kaltsoyannis and P. L. Arnold, Metal-metal bonding in uranium-group 10 complexes, *J. Am. Chem. Soc.*, 2016, **138**, 3333–3345.

92 S. Fortier, J. R. Aguilar-Calderon, B. Vlaisavljevich, A. J. Metta-Magana, A. G. Goos and C. E. Botez, An N-tethered uranium(III) arene complex and the synthesis of an unsupported U-Fe bond, *Organometallics*, 2017, **36**, 4591–4599.

93 E. Lu, A. J. Wooles, M. Gregson, P. J. Cobb and S. T. Liddle, A very short uranium(IV)-rhodium(I) bond with net double-dative bonding character, *Angew. Chem., Int. Ed.*, 2018, **57**, 6587–6591.

94 W. Fang, Q. Zhu and C. Zhu, Recent advances in heterometallic clusters with f-block metal-metal bonds: synthesis, reactivity and applications, *Chem. Soc. Rev.*, 2022, **51**, 8434–8449.

95 J. A. Hlina, J. A. L. Well, J. R. Pankhurst, J. Love and P. L. Arnold, Uranium rhodium bonding in heterometallic complexes, *Dalton Trans.*, 2017, **46**, 5540–5545.

96 O. P. Lam, C. Anthon, F. W. Heinemann, J. M. O'Connor and K. Meyer, Structural and spectroscopic characterization of a charge-separated uranium benzophenone ketyl radical complex, *J. Am. Chem. Soc.*, 2008, **130**, 6567–6576.

97 S. Harder and F. Feil, Dimeric benzylcalcium complexes: influence of THF in stereoselective styrene polymerization, *Organometallics*, 2002, **21**, 2268–2274.

98 J. A. Hermann and J. F. Suttle, Uranium(IV) chloride, *Inorg. Synth.*, 1957, **5**, 143–144.

99 O. V. Dolomanov, L. J. Bourhis, R. J. Gildea, J. A. K. Howard and H. Puschmann, OLEX2: a complete structure solution, refinement and analysis program, *J. Appl. Crystallogr.*, 2009, **42**, 339–341.

100 L. J. Bourhis, O. V. Dolomanov, R. J. Gildea, J. A. K. Howard and H. Puschmann, The anatomy of a comprehensive constrained, restrained refinement program for the modern computing environment-Olex2 dissected, *Acta Crystallogr., Sect. A: Found. Adv.*, 2015, **71**, 59–75.

101 G. M. Sheldrick, A short history of SHELX, *Acta Crystallogr., Sect. A: Found. Crystallogr.*, 2008, **64**, 112–122.